

Figure S1 (Related to STAR Methods). Magnetic resonance imaging (MRI).

Outer panels show sagittal plane T1 magnetic resonance images for the subjects contributing hippocampal tissue to the analysis. The location of anterior (orange) and posterior (blue) specimens obtained along the hippocampal axis are highlighted. Line segments represent approximately 3 cm of distance on the included images. The cartoon image shows a coronal section of the human brain indicating the position of the uncal apex, the posterior extent of which was used as a demarcation point for the anterior hippocampus. This structure can be identified relative to the oculomotor nerve and posterior cerebral artery in the ambient cistern, as shown in the cartoon.

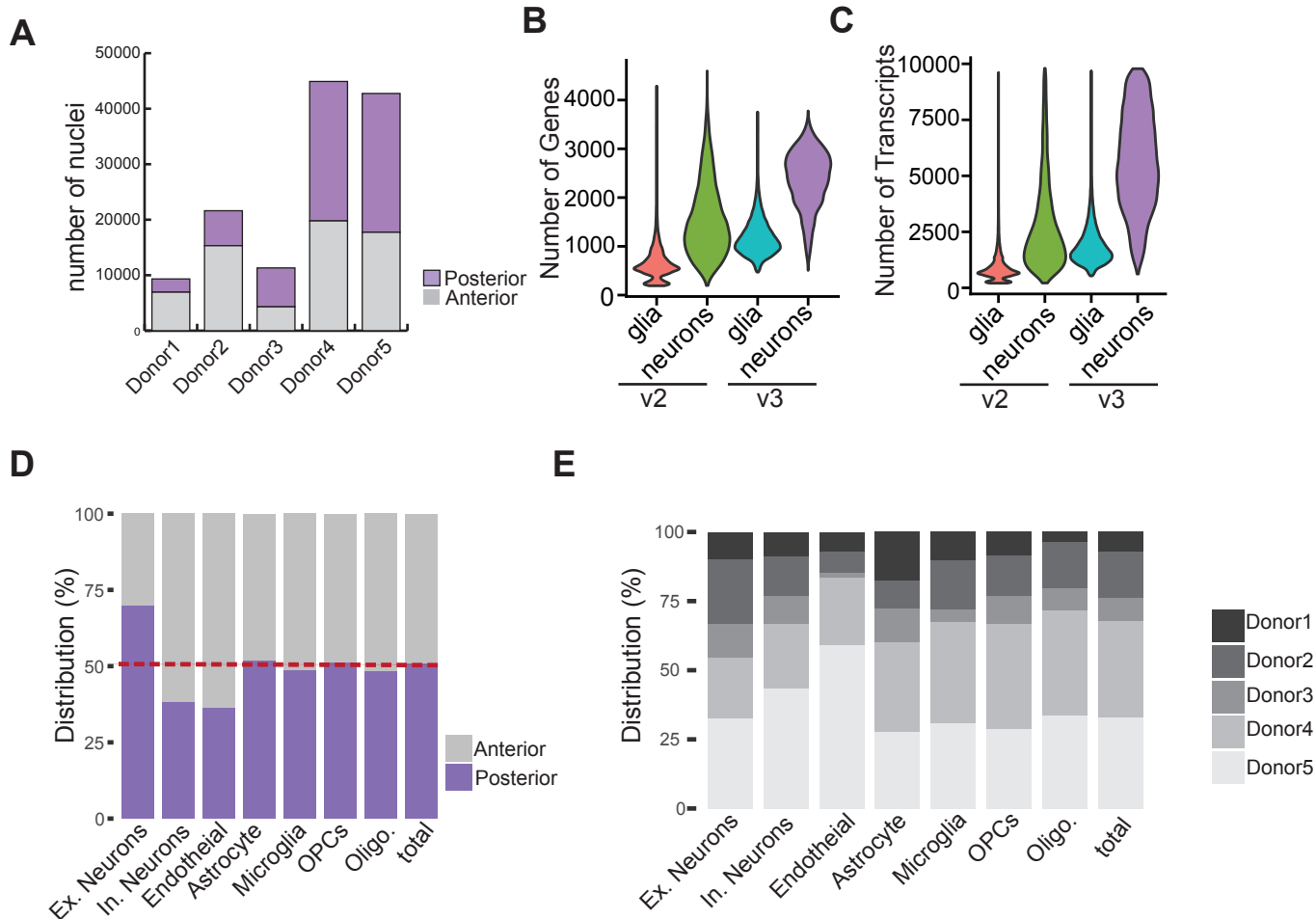


Figure S2 (Related to Figure 1). Data quality.

(A) Bar chart showing the number of nuclei sampled from each donor.

(B) Violin plots showing the distribution of the number of genes in glial and neuronal cells separated by 10X Genomics chemistry versions used (v2 or v3).

(C) Violin plot showing the distribution of the number of transcripts in glial and neuronal cells separated by 10X Genomics chemistry version used.

(D) Bar charts showing the distribution of anterior and posterior nuclei in cell-type identified.

(E) Distribution of nuclei obtained from individual donors.

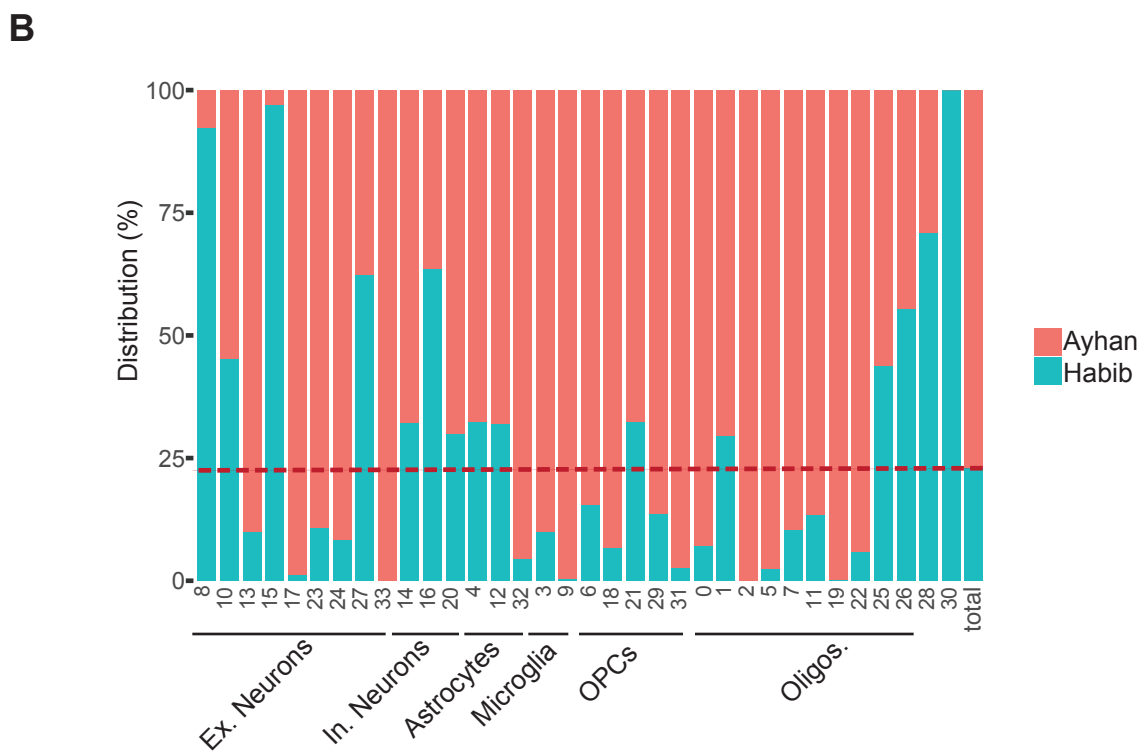
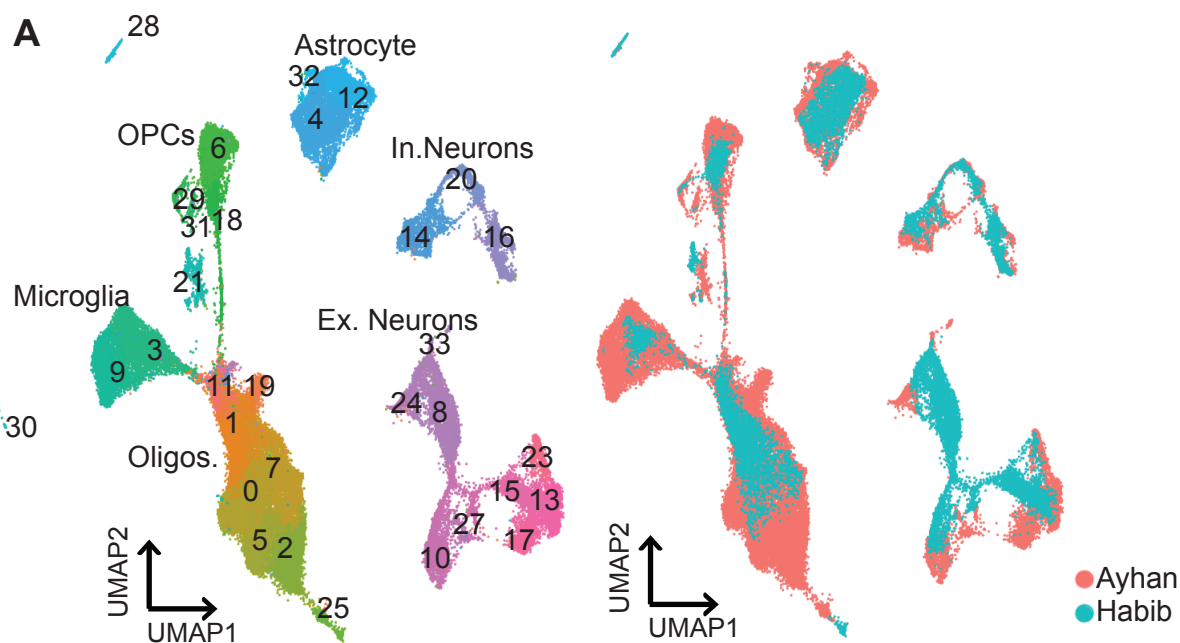


Figure S3 (Related to Figure 1). Integration of published human hippocampus dataset with our data.

(A) UMAP projections showing the clustering of a subset of our data combined with a published human hippocampus dataset (Habib et al., 2017) labeled by cluster annotations (left) and dataset (right).

(B) Bar plots showing the distribution of cells from our study and Habib et al. for each cluster.

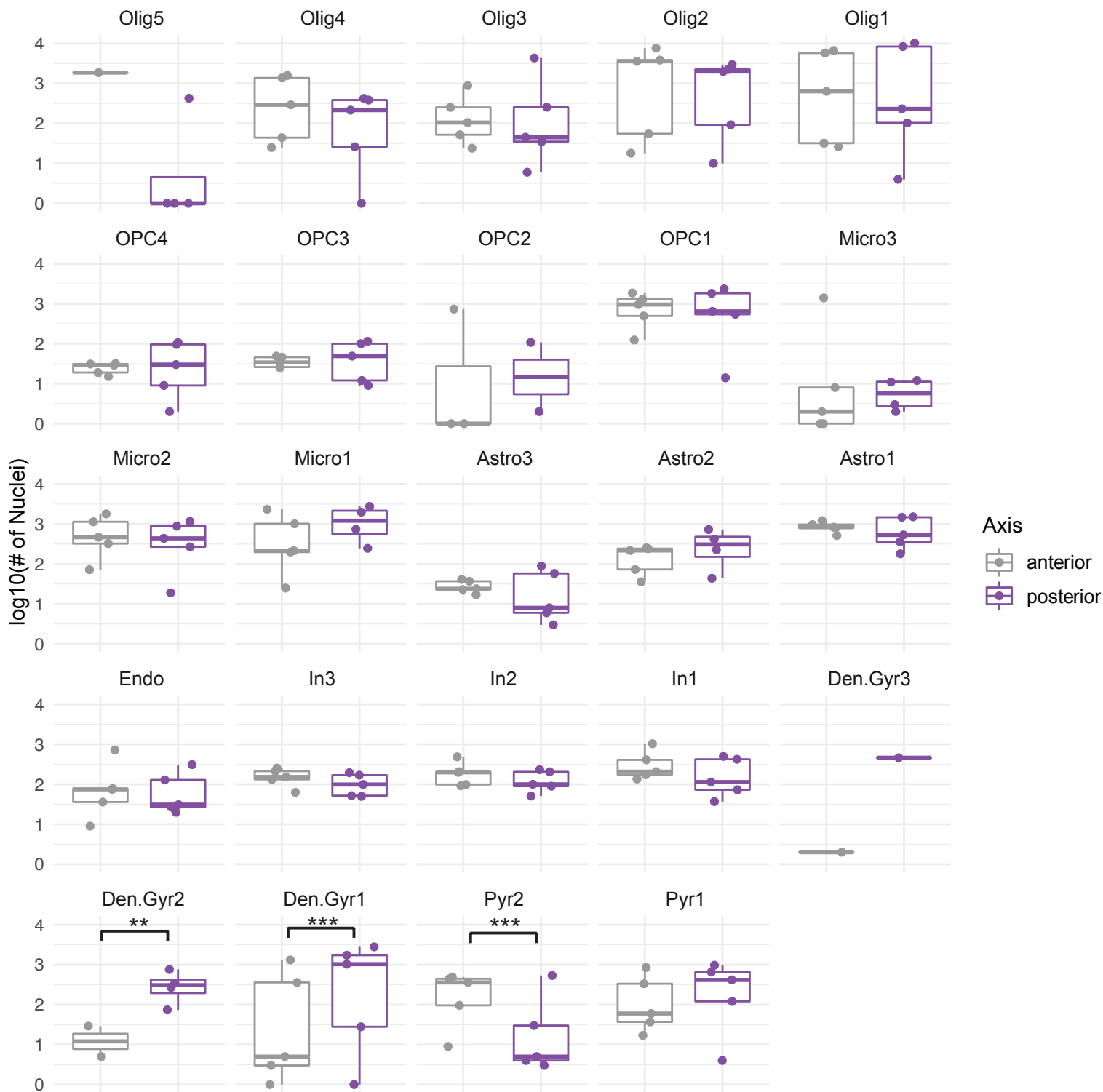


Figure S4 (Related Figure 1). Anterior vs. posterior distribution in clusters.

Boxplots depicting the anterior:posterior cell proportions for each cluster. Each data point is a donor. Colors correspond to the axis. ** $P < 0.01$, *** $P < 0.001$, Robust generalized mixed model. Clusters showing anterior or posterior enrichment driven by single donor (i.e Olig5, OPC2, Den.Gyr3) were not considered significant. Pyr=Pyramidal neurons, Den.Gyr=dentate gyrus neurons, In=Interneurons, Endo=endothelial cells, Micro=microglia, Astro=astrocytes, OPCs=oligodendrocyte progenitor cells, and Olig=oligodendrocytes.

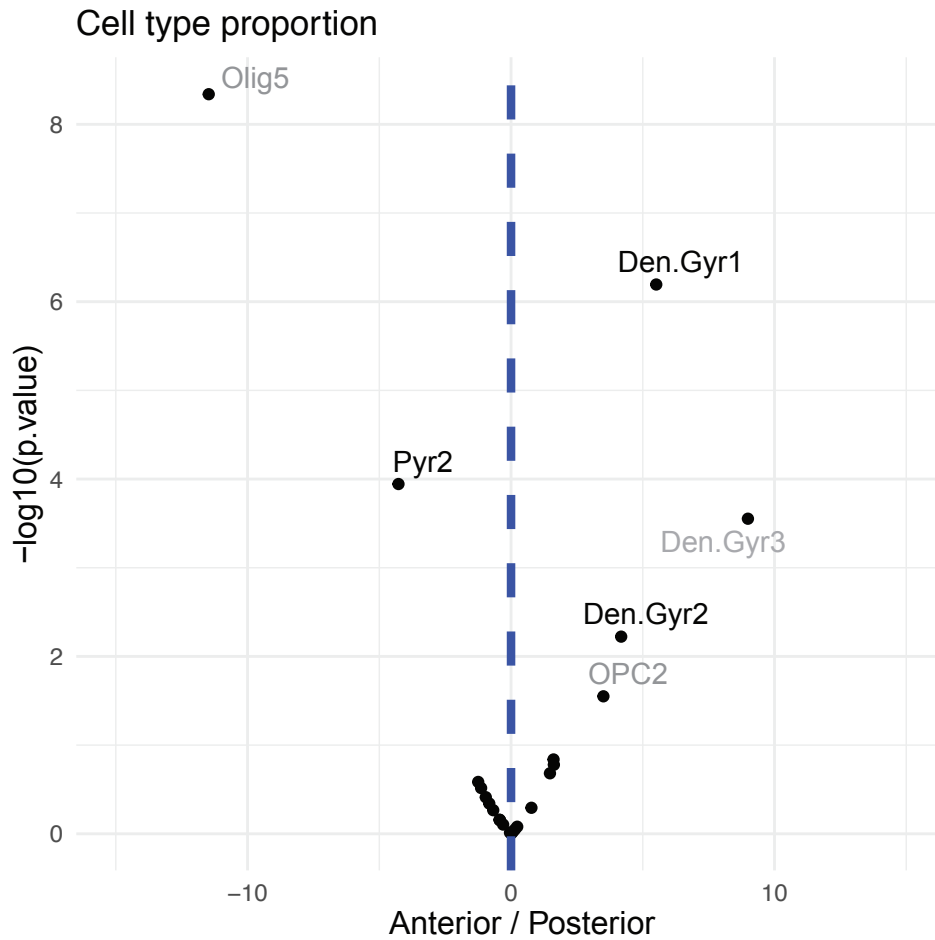


Figure S5 (Related to Figure 1). Statistics for anterior vs. posterior distribution in clusters.

Volcano plot depicting the cell type differential abundance between axis. X-axis corresponds to the robust mixed model estimates. Y-axis corresponds to the $-\log_{10}(\text{p-value})$. Pyr=Pyramidal neurons, Den.Gyr=dentate gyrus neurons. Clusters labeled driven by a single (OPC2, Olig5, and Den.Gyr3) are labeled gray.

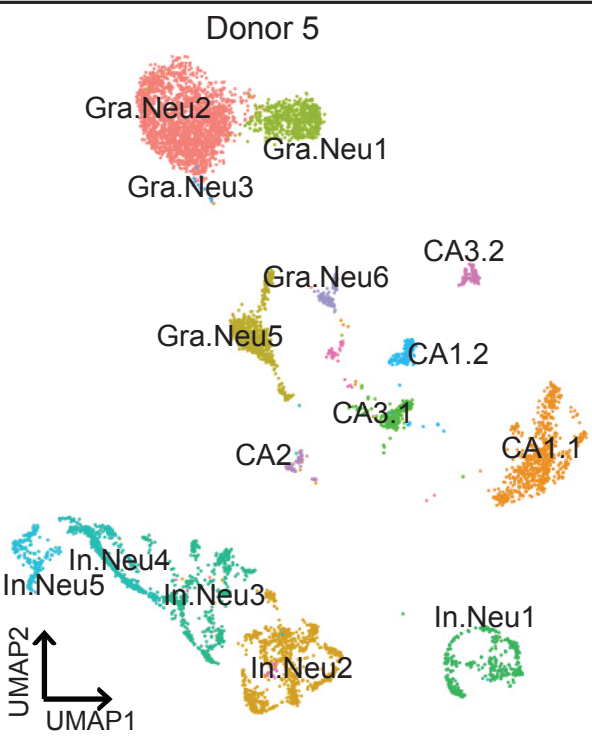
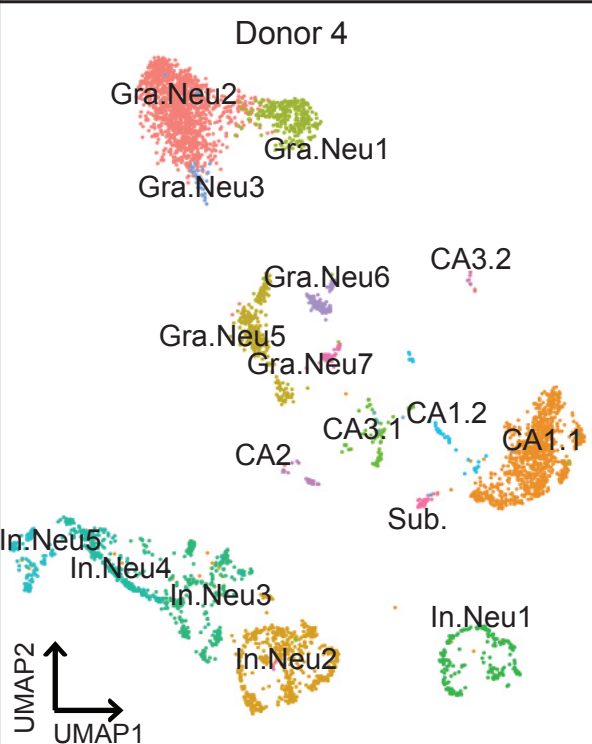
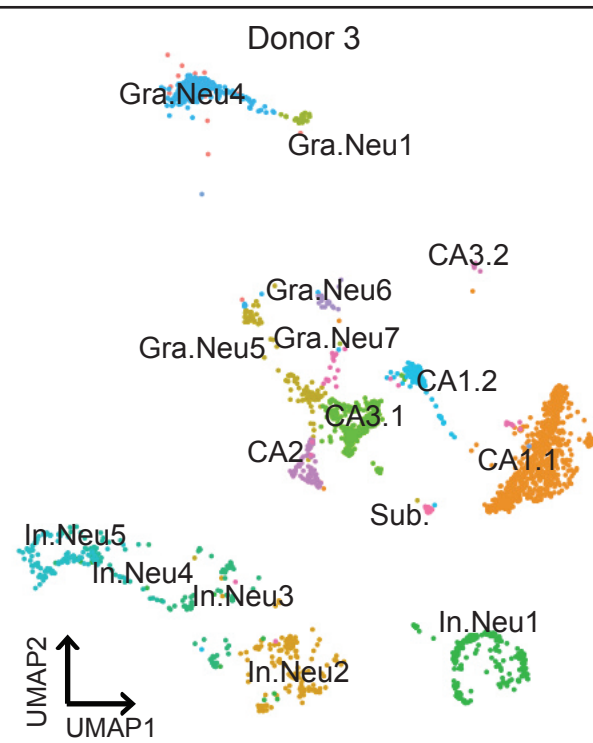
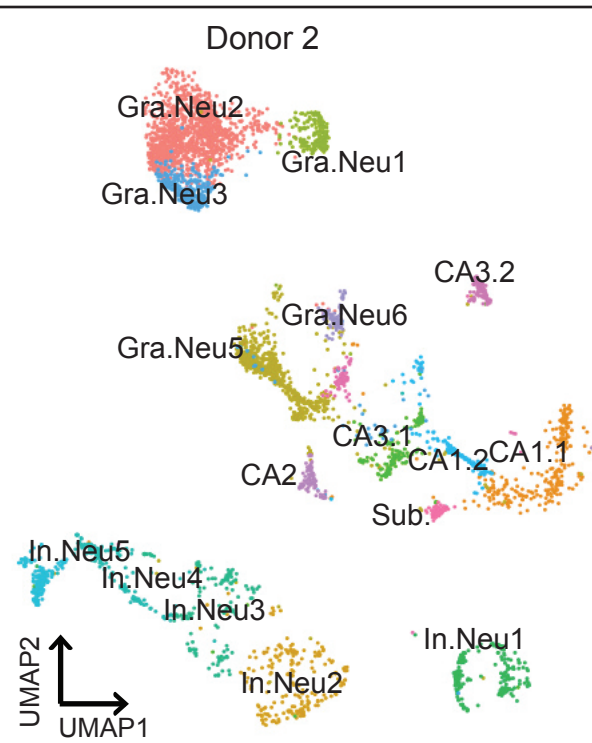
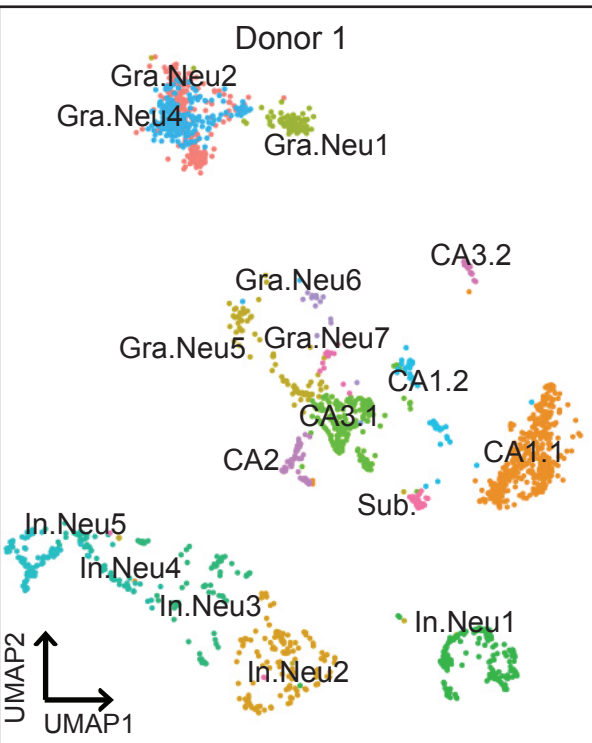


Figure S6 (Related to Figure 2). Neuronal clusters by donors.

UMAP plots showing neuronal clusters separated by corresponding donor tissue with cell type annotations.

Gra.Neu=Granule Neurons, In.Neu=Inhibitory neurons, and Sub=subiculum.

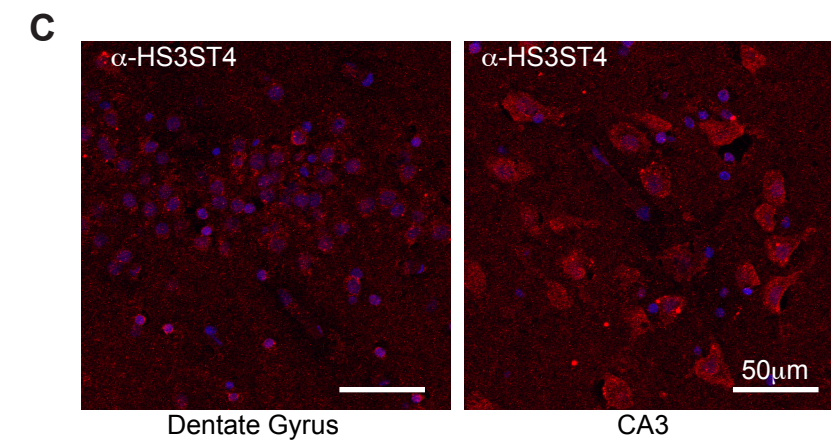
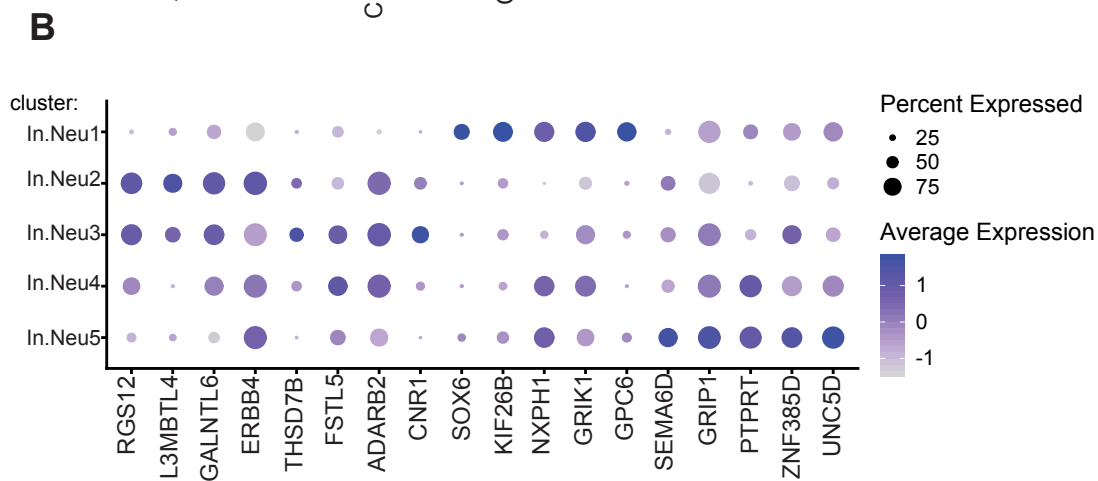
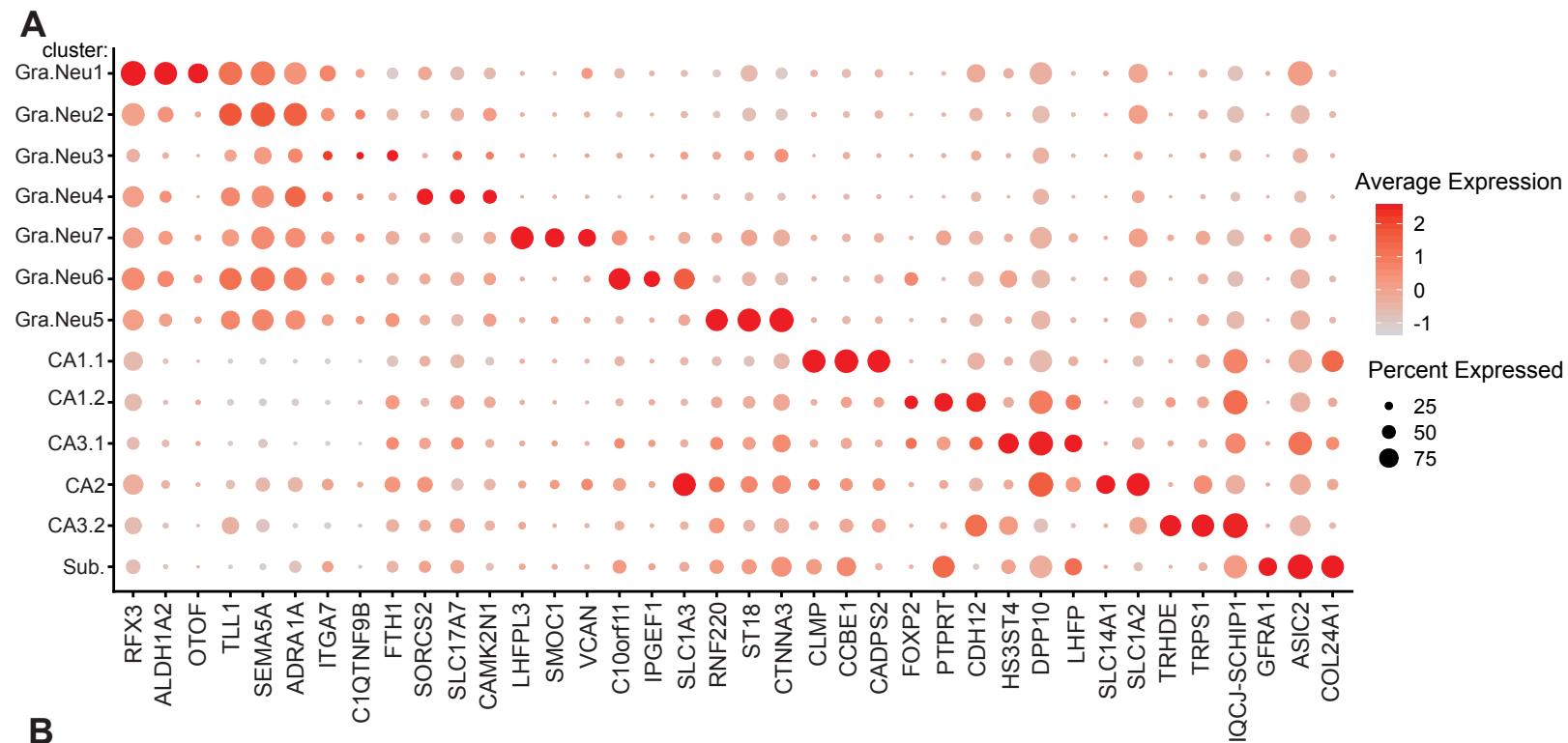


Figure S7 (Related to Figure 2). Identification and validation of neuronal cluster markers.

(A) Dot plots showing the top 3 cluster markers in excitatory neuronal clusters.

(B) Dot plots showing the top 5 cluster markers in inhibitory neuronal clusters.

(C) Immunohistochemistry showing HS3ST4 expression in CA3 subfield of human postmortem hippocampus. Blue color indicates the nuclear stain DAPI and red color shows α -HS3ST4 staining detected with a fluorophore conjugated antibody.

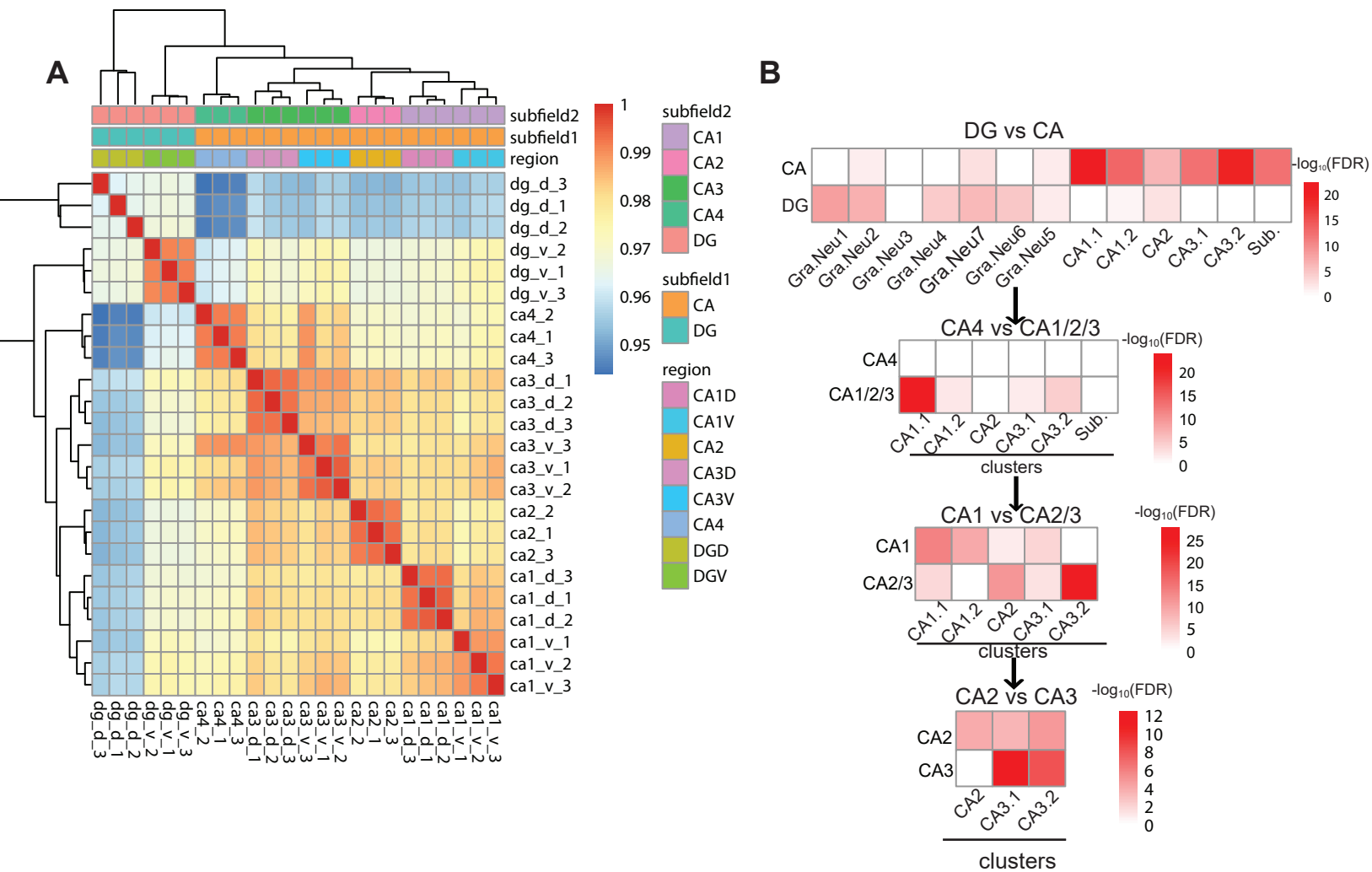


Figure S8 (Related to Figure 2). Annotation of excitatory clusters.

(A) Dendrogram depicting the hierarchical structure of gene expression of the hippocampal subfields in the Hipposeq dataset (Cembrowski et al., 2016b).

(B) Hypergeometric overlaps of excitatory neuronal clusters with mouse subfield markers identified via bulk RNA-seq (Cembrowski et al., 2016b). Heat map illustrates the $-\log_{10}(\text{FDR})$ of gene set enrichment between the markers of the human excitatory neuronal clusters and the gene set lists distinguishing CA vs DG, CA4 vs CA1/2/3, CA1 vs CA2/3, and CA2 vs CA3 in mouse. The x-axis lists the excitatory neuronal clusters and y-axis lists the mouse subfields.

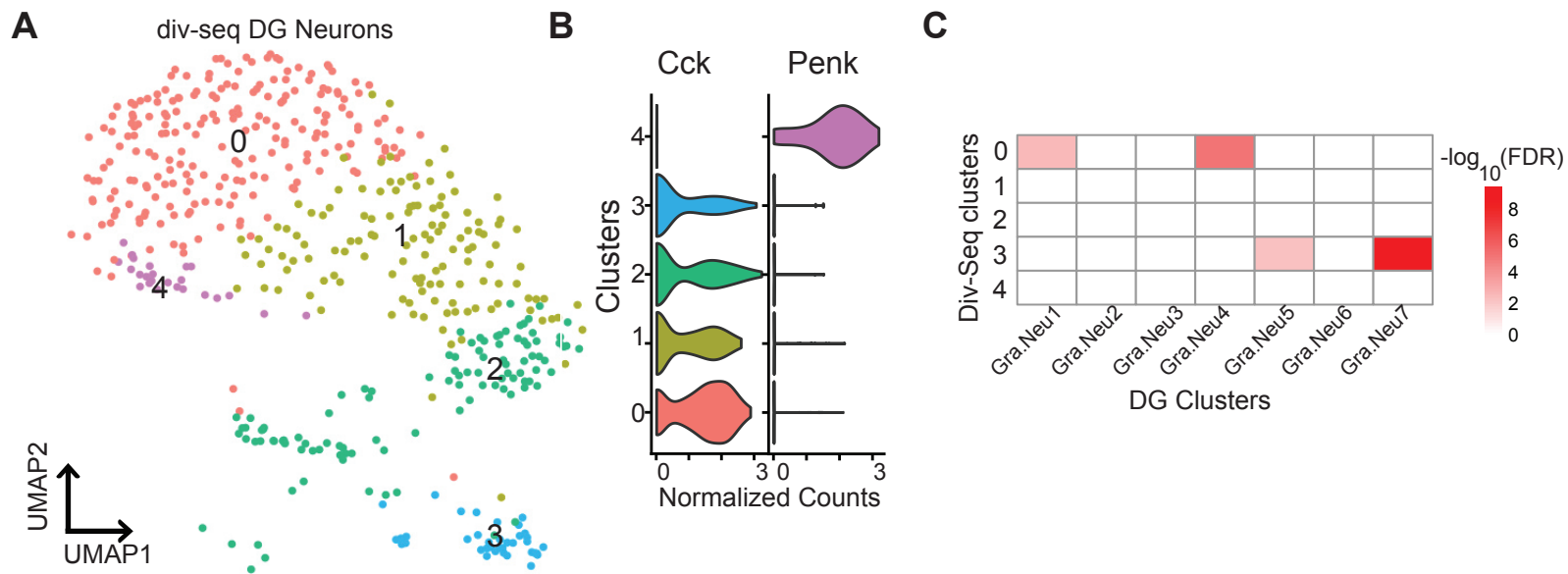


Figure S9 (Related to Figure 2). Human and mouse DG populations.

(A) UMAP plot of div-seq (Habib et al., 2016) dentate gyrus neuronal cells colored by cluster identities.

(B) Violin plots showing normalized counts for Cck and Penk showing DG populations identified by Erwin et al. (Erwin et al., 2020).

(C) Heatmap showing $-\log_{10}(\text{FDR})$ from a hypergeometric enrichment test for the overlaps between the marker genes for DG granule neuron clusters identified in our human dataset study and the marker genes div-seq DG granule neuron clusters.

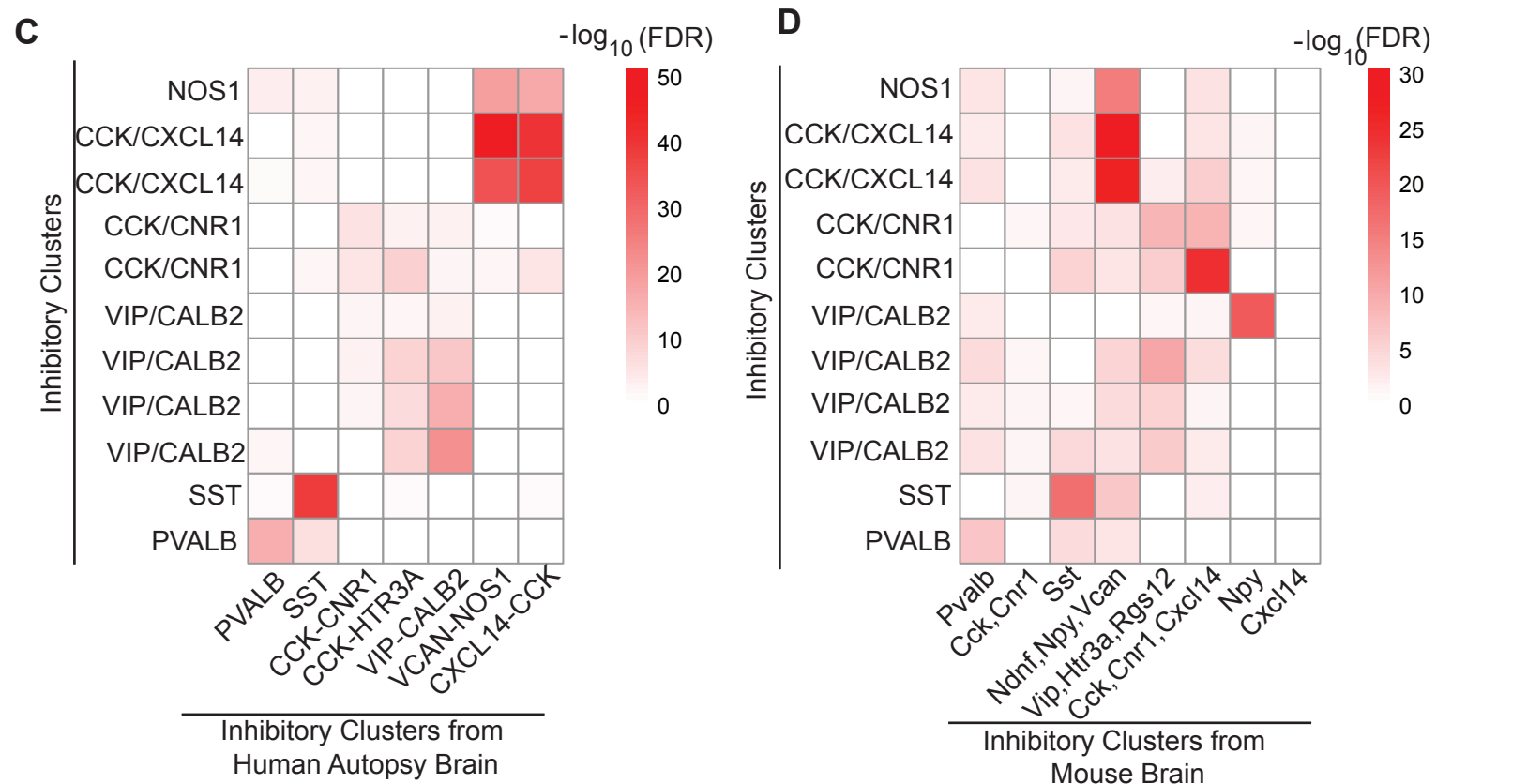
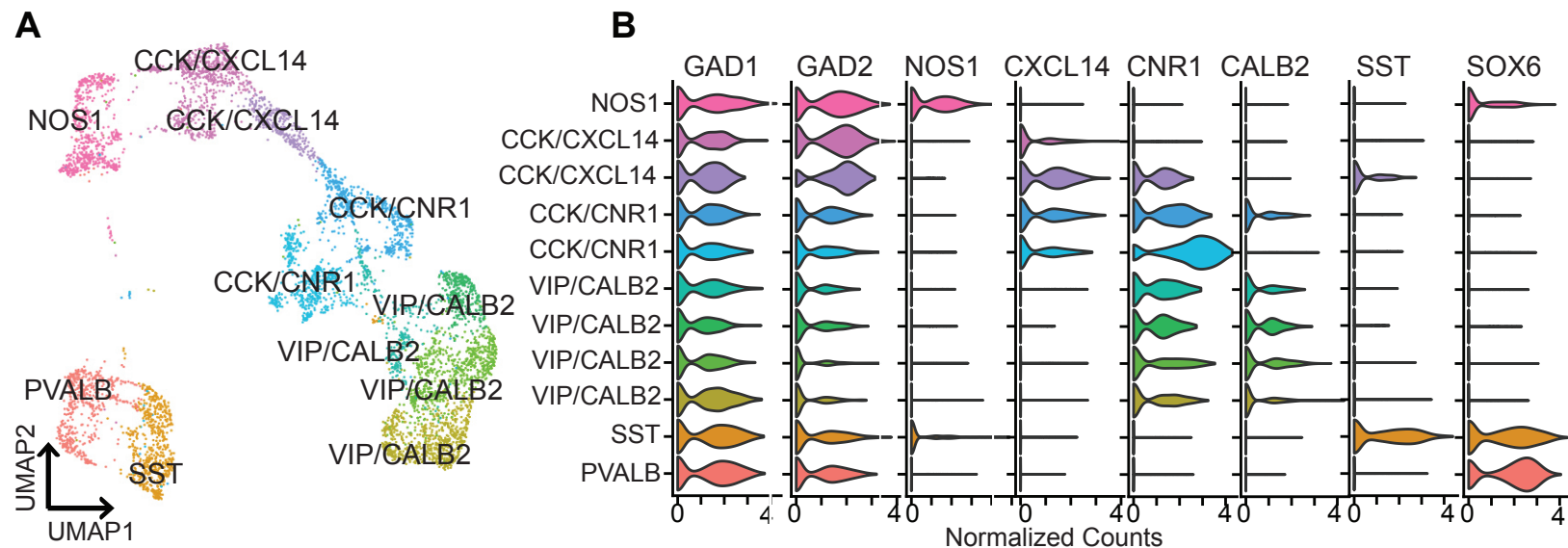


Figure S10 (Related to Figure 2). snRNA-seq reveals hippocampal GABAergic interneurons.

(A) UMAP plot of inhibitory neuronal cells colored by cluster identities and cell-type annotations.

(B) Violin plots showing normalized counts for interneuron markers.

(C) Heatmap showing $-\log_{10}(\text{FDR})$ from a hypergeometric enrichment test for the overlaps between the marker genes for inhibitory neuronal clusters identified in this study and the marker genes for inhibitory neuronal clusters identified in human autopsy brains by Habib et al. (Habib et al., 2017).

(D) Heatmap showing $-\log_{10}(\text{FDR})$ from a hypergeometric enrichment test for the overlaps between the marker genes for inhibitory neuronal clusters identified in this study and the marker genes for inhibitory neuronal clusters identified in mouse hippocampus by Habib et al. (Habib et al., 2017).

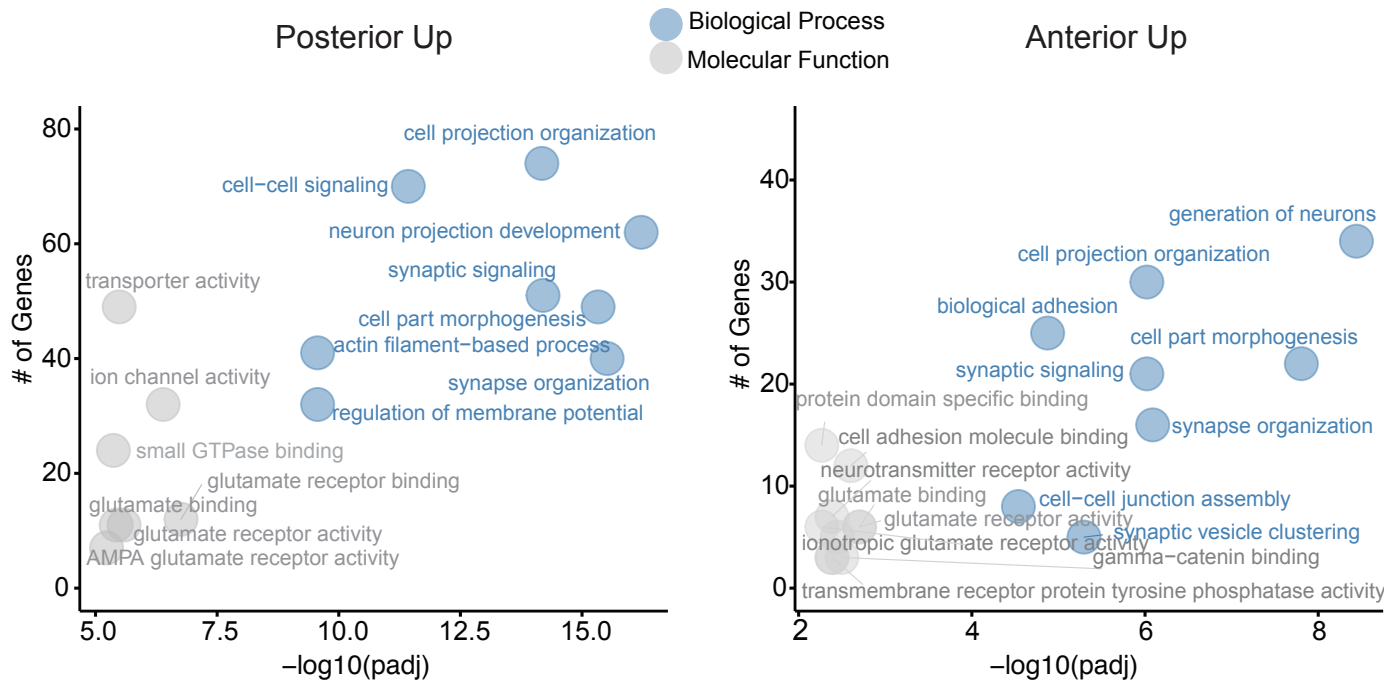


Figure S11 (Related to Figure 3). Gene ontology analysis of CA1-specific DEGs.

Bubble chart showing the top gene ontology categories for genes with higher expression in posterior (left) and anterior (right) hippocampus. On the x-axis is the $-\log_{10}(\text{FDR})$ and on the y-axis is the number of genes per category. BP (blue)=biological function; MF (gray)=molecular function.

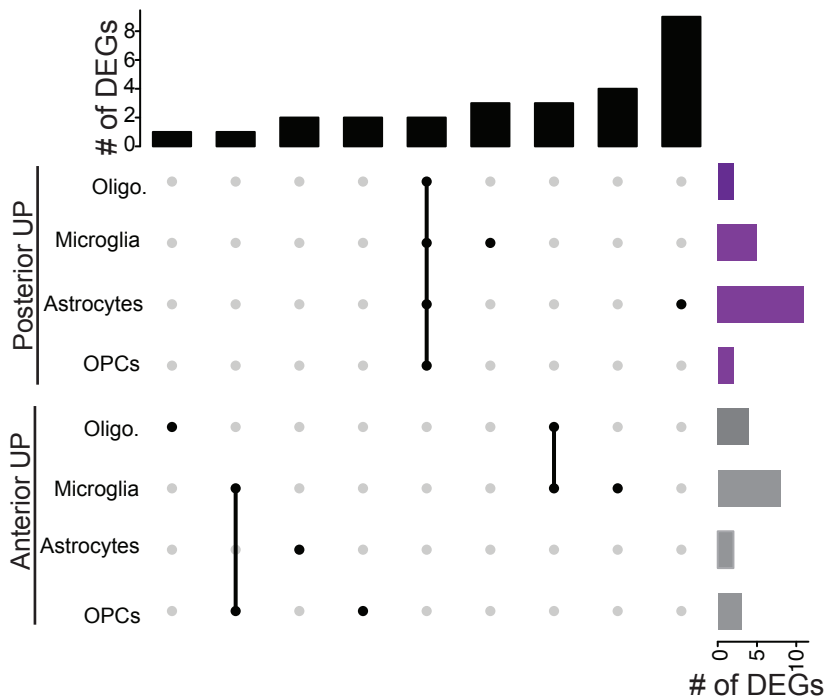


Figure S12 (Related to Figure 6). Glial specific DEGs across anterior and posterior hippocampus.

Upset plot showing the overlap of upregulated or downregulated DEGs in glial cell-types across aHP and pHP (adj. p-value<0.05, log2FC>0.3, percentage>25). Horizontal bars show the number of genes enriched in posterior (purple) and anterior (gray) in each cell type. Vertical black bars show the number of overlapping DEGs across the glial cell types. Oligo.=Oligodendrocytes

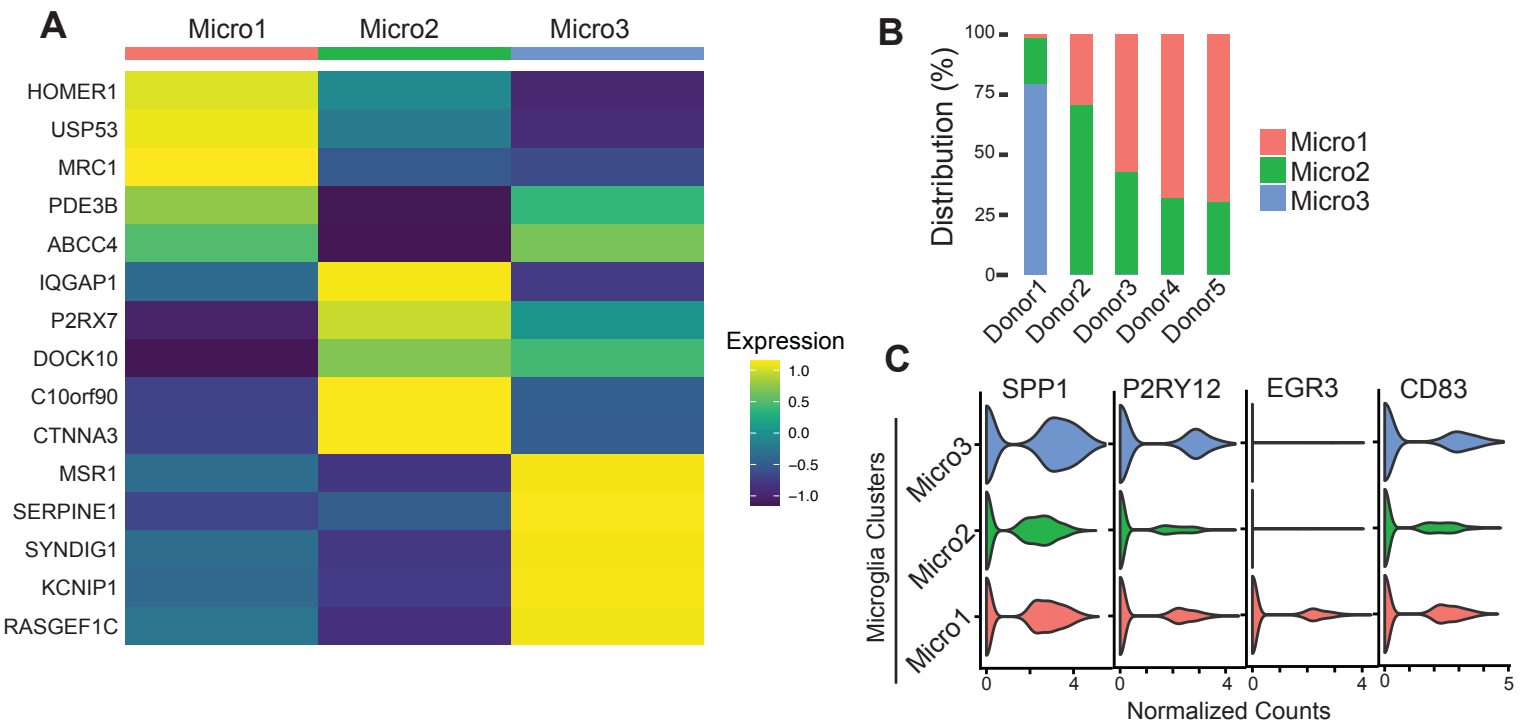
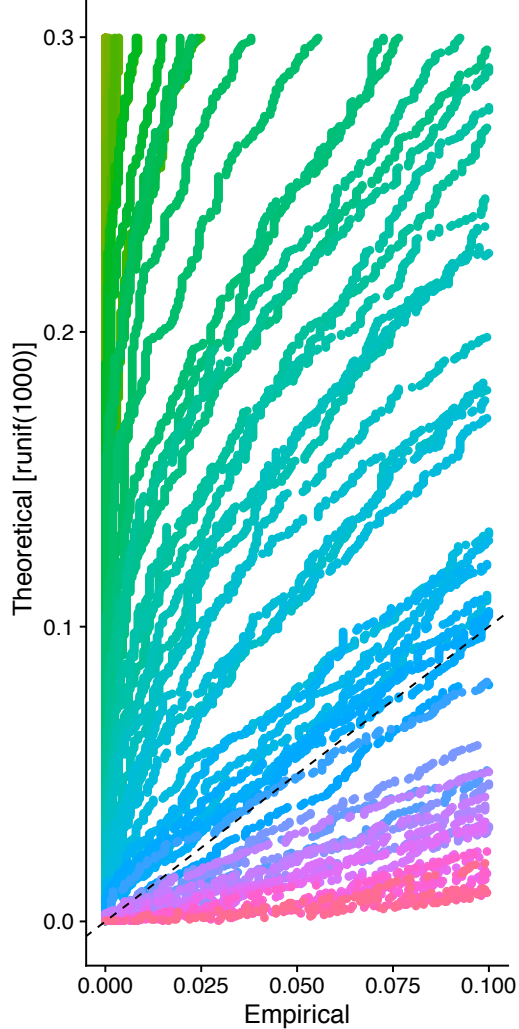


Figure S13 (Related to Figure 6). Microglia gene expression in human hippocampus.

(A) Heatmap illustrating the average expression of the top 5 DEGs between microglia clusters. Color scheme corresponds to log-normalized and scaled values for average gene expression for each cluster

(B) Frequency distribution of microglia clusters in five donors.

(C) Violin plots showing the expression of homeostatic and pre-active microglia.

A

PC: p-value

PC 1: 0	PC 21: 1.65e-182	PC 41: 1.28e-30	PC 61: 0.00438	PC 81: 1
PC 2: 0	PC 22: 8.75e-260	PC 42: 5.75e-23	PC 62: 0.00438	PC 82: 1
PC 3: 0	PC 23: 2.07e-136	PC 43: 6.45e-13	PC 63: 0.0005	PC 83: 1
PC 4: 0	PC 24: 2.24e-233	PC 44: 3.98e-27	PC 64: 0.000172	PC 84: 1
PC 5: 0	PC 25: 4.01e-164	PC 45: 2.8e-14	PC 65: 0.479	PC 85: 1
PC 6: 0	PC 26: 1.55e-142	PC 46: 7.97e-14	PC 66: 0.133	PC 86: 1
PC 7: 2.03e-259	PC 27: 2.2e-134	PC 47: 1.59e-19	PC 67: 0.133	PC 87: 1
PC 8: 0	PC 28: 9.98e-114	PC 48: 3.83e-13	PC 68: 0.479	PC 88: 1
PC 9: 0	PC 29: 1.61e-99	PC 49: 5.19e-17	PC 69: 0.133	PC 89: 1
PC 10: 0	PC 30: 1.22e-76	PC 50: 3.75e-08	PC 70: 1	PC 90: 1
PC 11: 4.41e-251	PC 31: 1.72e-58	PC 51: 1.09e-12	PC 71: 1	PC 91: 1
PC 12: 0	PC 32: 5.02e-87	PC 52: 2.49e-06	PC 72: 0.248	PC 92: 1
PC 13: 0	PC 33: 1.44e-92	PC 53: 4.64e-09	PC 73: 1	PC 93: 1
PC 14: 0	PC 34: 6.12e-49	PC 54: 0.00253	PC 74: 0.479	PC 94: 1
PC 15: 0	PC 35: 1.83e-63	PC 55: 0.248	PC 75: 0.133	PC 95: 1
PC 16: 3.52e-290	PC 36: 3.99e-76	PC 56: 5.92e-05	PC 76: 0.0411	PC 96: 1
PC 17: 1.29e-261	PC 37: 1.71e-36	PC 57: 0.0132	PC 77: 0.479	PC 97: 1
PC 18: 4.96e-266	PC 38: 1.12e-37	PC 58: 0.133	PC 78: 1	PC 98: 1
PC 19: 2.05e-184	PC 39: 2e-49	PC 59: 0.00253	PC 79: 1	PC 99: 1
PC 20: 1.08e-254	PC 40: 9.95e-48	PC 60: 0.000172	PC 80: 1	PC 100: 1

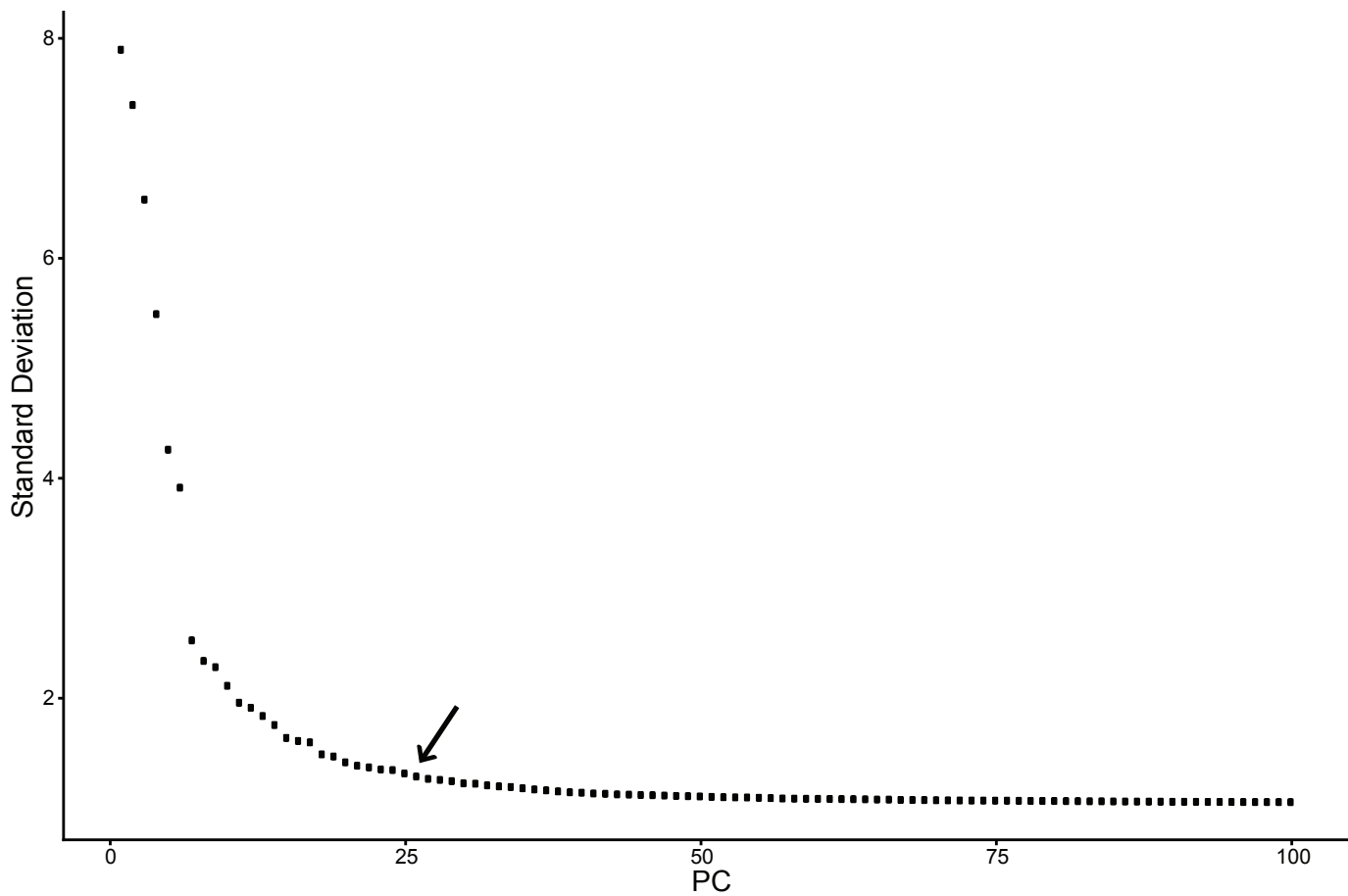
B

Figure S14 (Related to STAR Methods). JackStraw and Elbow Plots of the entire dataset.

(A) Scatter plot showing JackStraw statistics for each of the principal component (1-100) for PCA significance for dataset shown in Figure 1.

(B) Scree plot (Elbow Plot) showing the ranking of principle components based on the percentage of variance explained by each one for dataset shown in Figure 1. Arrow shows flattening around PC 25.

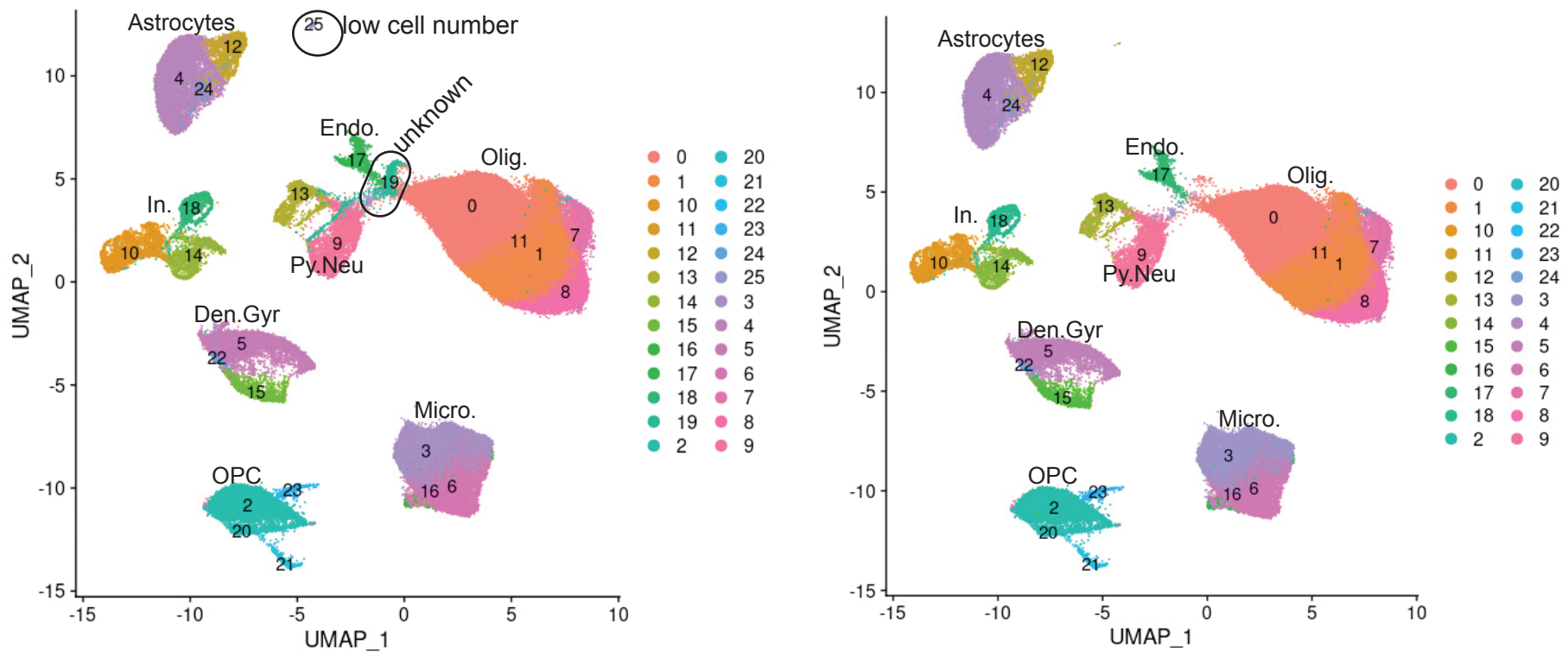
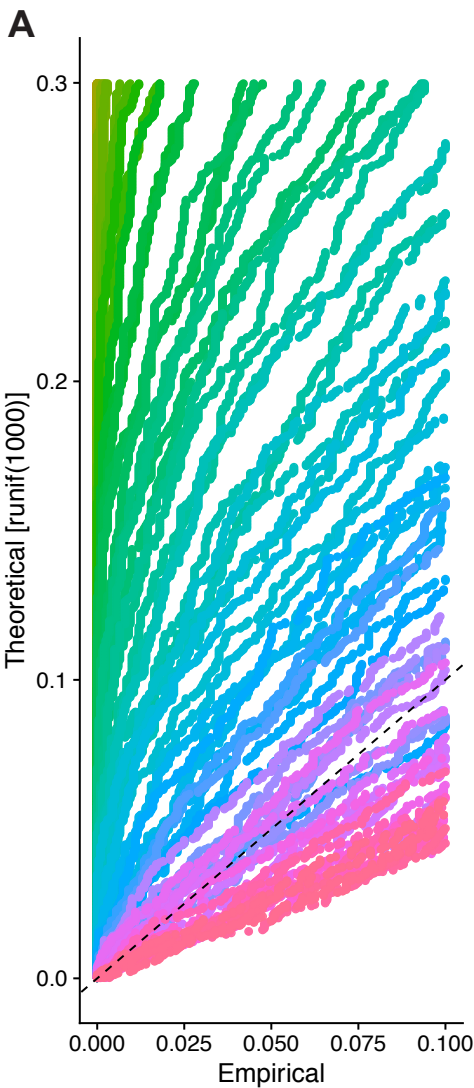


Figure S15 (Related to STAR Methods). Filtered clusters from entire dataset.

UMAP plot showing clustering the entire dataset with removed clusters labeled (left). UMAP plot final clustering after removal of two clusters (right). Py.Neu=Pyramidal neurons, Den.Gyr=dentate gyrus neurons, In=Interneurons, Astro=Astrocytes, Endo=endothelial cells, Micro=microglia, OPCs=oligodendrocyte progenitor cells, and Olig=oligodendrocytes.



PC: p-value

PC 1: 0	PC 21: 1.49e-147	PC 41: 3.97e-21	PC 61: 0.00438	PC 81: 0.0411
PC 2: 0	PC 22: 6.06e-159	PC 42: 3.4e-33	PC 62: 0.0232	PC 82: 0.479
PC 3: 0	PC 23: 7.32e-138	PC 43: 2.33e-27	PC 63: 2.05e-05	PC 83: 0.248
PC 4: 0	PC 24: 2.16e-104	PC 44: 9.83e-15	<u>PC 64: 0.000101</u>	PC 84: 1
PC 5: 0	PC 25: 9.19e-109	PC 45: 1.84e-12	PC 65: 0.133	PC 85: 1
PC 6: 0	PC 26: 1.35e-144	PC 46: 7.97e-14	PC 66: 0.0132	PC 86: 1
PC 7: 1.41e-243	PC 27: 7.86e-122	PC 47: 3.75e-08	PC 67: 0.0735	PC 87: 1
PC 8: 8.02e-320	PC 28: 9.39e-106	PC 48: 3.38e-23	PC 68: 0.133	PC 88: 1
PC 9: 1.59e-204	PC 29: 6.38e-90	PC 49: 1.63e-09	PC 69: 0.00759	PC 89: 0.479
PC 10: 3.29e-229	PC 30: 2.3e-83	PC 50: 2.75e-09	PC 70: 1	PC 90: 1
PC 11: 5.27e-281	PC 31: 1.79e-79	PC 51: 5.22e-12	PC 71: 1	PC 91: 1
PC 12: 9.74e-270	PC 32: 6.77e-77	PC 52: 3.05e-07	PC 72: 0.248	PC 92: 1
PC 13: 4.71e-255	PC 33: 4.87e-46	PC 53: 0.00147	PC 73: 0.248	PC 93: 1
PC 14: 1.81e-273	PC 34: 5.28e-41	PC 54: 8.78e-17	PC 74: 0.479	PC 94: 1
PC 15: 2.76e-249	PC 35: 8.18e-54	PC 55: 3.75e-08	PC 75: 0.479	PC 95: 1
PC 16: 4.18e-226	PC 36: 5.7e-61	PC 56: 0.000172	PC 76: 0.479	PC 96: 1
PC 17: 4.44e-193	PC 37: 2.65e-54	PC 57: 0.000293	PC 77: 0.0411	PC 97: 1
PC 18: 2.87e-219	PC 38: 1.4e-24	PC 58: 0.000172	PC 78: 0.479	PC 98: 1
PC 19: 1.83e-191	PC 39: 1.98e-33	PC 59: 2.49e-06	PC 79: 0.0132	PC 99: 1
PC 20: 1.11e-161	PC 40: 2.38e-24	PC 60: 3.48e-05	PC 80: 0.0735	PC 100: 0.248

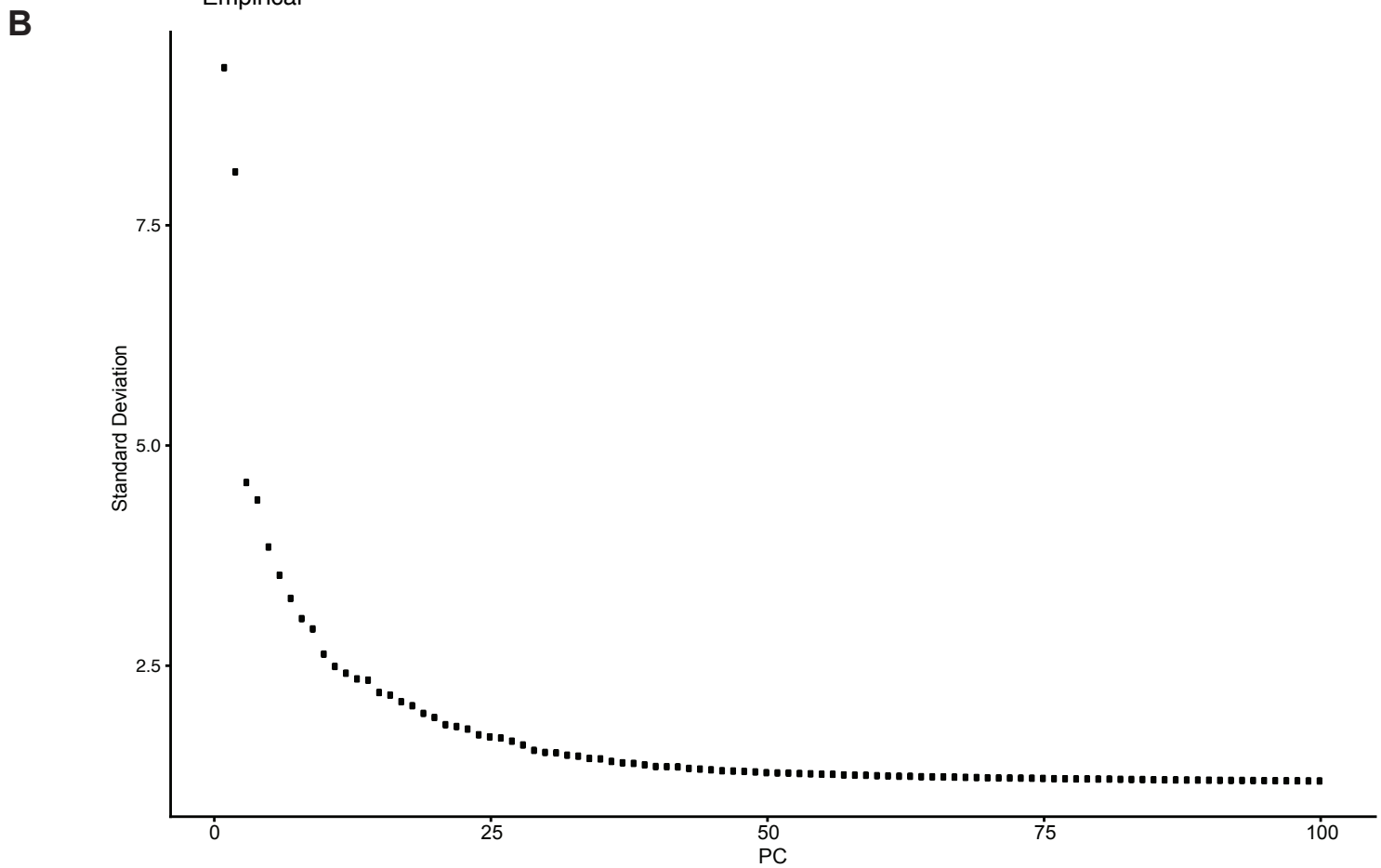


Figure S16 (Related to STAR Methods). JackStraw and Elbow Plots of the neuronal cells.

(A) Scatter plot showing JackStraw statistics for each of the principal component (1-100) for PCA significance for dataset shown in Figure 2.

(B) Scree plot (Elbow Plot) showing the ranking of principle components based on the percentage of variance explained by each one for dataset shown in Figure 2.

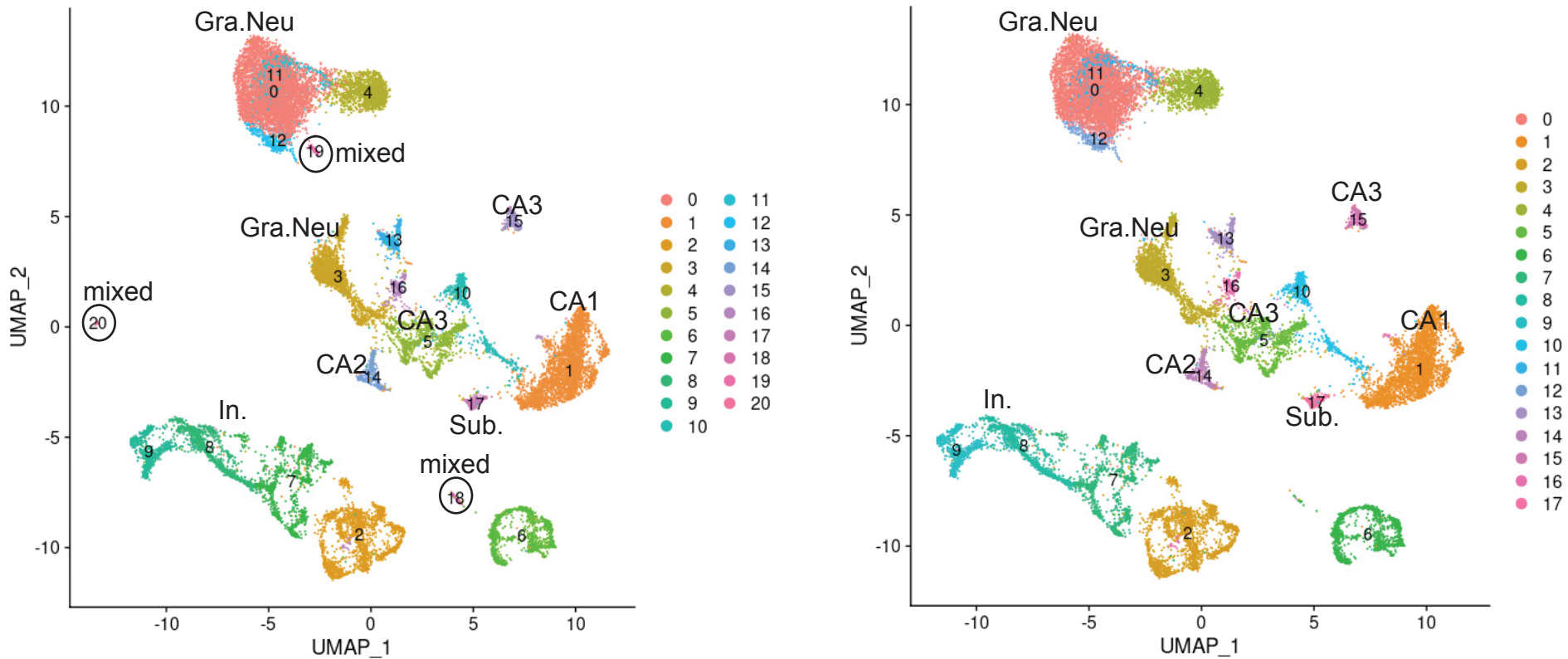


Figure S17 (Related to STAR Methods). Filtered neuronal clusters.

UMAP plot showing neuronal clustering with removed clusters labeled (left). UMAP plot final clustering after removal of three clusters (right).

Gra.Neu=Granule Neurons, In=Inhibitory neurons, and Sub=subiculum.

Figure S18 (Related to STAR Methods). Variance explained by covariates.

(A) Bar plot depicting the variance explained by each covariate. Y-axis represent the variance explained weighted across the first 10 PCs.

(B) Bar plot depicting the variance explained by each covariate for each cluster. Clusters defined by one subject (Olig5, Den.Gyr3, OPC2, Micro3) were removed from the analysis. Y-axis represent the variance explained weighted across the first 10 PCs.